Diffuse correlation spectroscopy with oximetry disentangles the efficacy of cerebral blood flow during hypothermic circulatory arrests

Alexander I. Zavriyev[1], Kutlu Kaya[1], Parisa Farzam[1], Parya Y. Farzam[1], John Sunwoo[1], Felipe Orihuela-Espina[1, 4], Arminder S. Jassar[2], Duke E. Cameron[2], Thoralf M. Sundt[2], Serguei Melnitchouk[2], Stefan A. Carp[1], Maria Angela Franceschini[1], Jason Z. Qu[3]

1: Optics at Athinoula A. Martinos Center for Biomedical Imaging, Department of Radiology, Massachusetts General Hospital, Harvard Medical School, Boston, MA, USA

2: Division of Cardiac Surgery, Massachusetts General Hospital, Harvard Medical School, Boston, MA, USA

3: Department of Anesthesia, Critical Care and Pain Medicine, Massachusetts General Hospital, Harvard Medical School, Boston, MA, USA

4: Computational Sciences, Instituto Nacional de Astrofísica, Óptica y Electrónica (INAOE), Puebla, Mexico

Corresponding Author: Alexander Zavriyev, 149 13th Street, Charlestown, MA, 02129, 781-715-5058, zav.shurik@gmail.com.

Abstract

Real-time noninvasive monitoring of cerebral blood flow during surgery could improve the morbidity and mortality rates associated with hypothermic circulatory arrests (HCA) in adult cardiac patients. In this study, we used a combined frequency domain near-infrared spectroscopy (FDNIRS) and diffuse correlation spectroscopy (DCS) system to measure cerebral oxygen saturation (SO_2) and an index of blood flow (CBF_i) in 12 adults going under cardiac surgery with HCA. Our measurements revealed that a negligible amount of blood is delivered to the brain during HCA with retrograde cerebral perfusion (RCP), indistinguishable from HCA-only cases (CBF_i drops of 91.2% ± 3.3% and 95.5% ± 1.8%, respectively) and that CBF_i drops for both are significantly higher than drops during HCA with antegrade cerebral perfusion (ACP) ($p = 0.003$). We conclude that FDNIRS-DCS can be a powerful tool to optimize cerebral perfusion, and that RCP needs to be further examined to confirm its efficacy, or lack thereof.

Introduction

Neurologic injury is one of the most dreaded complications in cardiac surgery. Maintenance of optimal brain blood flow during cardiac surgery is an essential part of ensuring patients' neurological health. Among the cardiac surgical procedures, those imposing the greatest risk of neurologic injury include procedures requiring episodes of hypothermic circulatory arrest (HCA). Circulatory arrest (CA) involves cessation of all blood flow to the body, to allow surgeons to operate in a bloodless field (1). Hypothermia has been the mainstay of the surgical strategies to prevent cerebral ischemic injury during CA. This consists of using the cardiopulmonary bypass circuit to lower the patient's body temperature by circulating cold blood through the patient's body to achieve moderate (20.1 to 28°C) or deep (14.1 to 20°C) levels of hypothermia and reduce metabolic rate (1). By lowering the brain's metabolic rate, hypothermia reduces the need for oxygen delivery during CA. Under deep hypothermia, the brain can tolerate CA without clinically significant neurological injury for 30-40 minutes (5). However, hypothermia alone may not provide adequate brain protection for patients whose surgery requires more time, or during circulatory arrest under moderate hypothermia. Cerebral ischemia can result in both temporary injuries such as delirium and neurocognitive dysfunction, and

permanent brain injury, such as a stroke. Thus, it has become common clinical practice to provide cerebral perfusion to maintain blood flow to the brain during procedures requiring longer durations of CA. The most common methods are retrograde and antegrade cerebral blood perfusion (RCP and ACP, respectively) (6). During RCP, cold blood is delivered to the brain via retrograde flow in the venous system through a cannula placed in the superior vena cava. In selective ACP, the brain is perfused in an antegrade fashion via the arterial system, often unilaterally through the right axillary or the innominate artery.

While some studies have shown that adjunctive cerebral perfusion decreases the morbidity and mortality rates of aortic arch surgery, there is ongoing discussion regarding the best perfusion strategy for optimal neuroprotection during CA (7,8). This is due to the limited ability to monitor blood perfusion efficacy of these techniques. Currently available techniques for monitoring brain health in cardiac surgery procedures include electroencephalography (EEG) and cerebral oximeters using near-infrared spectroscopy (NIRS). While providing some insight on brain protection efficacy in real-time and helping fine-tune management strategies, these monitoring techniques each present some limitations. During deep hypothermic CA, EEG is used to ensure hypothermia and anesthesia are adequate to maintain the point of complete suppression of electrical activity, referred to as electrocerebral silence (9). Accordingly, functional damage cannot be detected. NIRS oximetry uses near-infrared light (generally 650 to 850 nm) to estimate regional oxygen saturation (rSO_2) in the brain (10); but it cannot distinguish between rSO_2 changes due to oxygen availability or consumption. A drop in NIRS readings may indicate a CBF drop, but it could also indicate sustained oxygen consumption as a result of insufficient hypothermia or anesthesia. The only currently available noninvasive CBF monitor is transcranial Doppler ultrasound (TCD), which measures blood flow velocity in the large basal arteries of the brain (11); however, TCD is not suited for long term monitoring, requiring stable positioning and alignment, and is very user dependent (12).

Diffuse correlation spectroscopy (DCS) is a noninvasive optical imaging technique that provides an index of cerebral blood flow (CBF_i) and has been shown to effectively monitor blood flow in cardiac surgical procedures in neonates pre- and/or postoperatively (13–15). It makes use of the speckle interference pattern formed when coherent light travels through a scattering medium. The pattern perturbs as the scattering centers drift, and by computing the intensity autocorrelation of speckles $g_2(\tau)$, one can estimate the velocity of moving scatterers (16). Since red blood cells form the overwhelming majority of moving scatterers in tissue, DCS provides a measure of blood flow index in the scalp, skull, and brain tissue. Studies have demonstrated that DCS is a useful tool for continuous monitoring of CBF (17,18) and holds promise for differentiating several pathological conditions such as ischemia and passive hyperemia (19). DCS measurements are conducted via a soft lightweight patch probe that can stay attached to the patient's head for however long is necessary, making it a strong candidate for use in the operating room. Further, it is possible to use both NIRS and DCS synergistically and acquire an index of cerebral metabolic rate of oxygen ($CMRO_{2i}$), a more comprehensive measure of brain health (20).

In this study, we use a hybrid instrument combining frequency-domain near-infrared spectroscopy (FDNIRS) and DCS to understand the course of cerebral perfusion during hypothermic circulatory arrest procedures in an adult population. We believe that our work proves the feasibility of acquiring both hemoglobin oxygenation (SO_2) and CBF_i

noninvasively during surgery and illustrates a potentially effective monitoring approach to reducing the perioperative neurological injury and subsequent morbidity and mortality in HCA procedures.

Materials and Methods

We enrolled twelve patients (7 male, 5 female, mean age 61.8 ± 19.4 years) scheduled to undergo elective cardiac surgery with use of circulatory arrest (4 HCA-only, 3 RCP, 5 ACP) between February 2017 and December 2019 at the Massachusetts General Hospital (MGH). Potential HCA patients were approached during their preoperative visit, between 3 and 10 days before the scheduled surgery. The study was explained to the patients by a physician and they had until the day of the surgery to decide whether to participate. All patients signed a written informed consent. This study was reviewed and approved by the Partners Healthcare Human Research Committee (IRB; #2016P001944). Table 1 outlines the patients' demographic distribution.

#	Age	Sex	Operative Procedure	Average HCA Temp (°C)	Cerebral perfusion	Circ Arrest duration	Optical Modality	INVOS NIRS Present	Probe Location (Forehead)	Monitoring Duration
1	57	M	Valve sparing aortic root replacement + Ascending aortic + hemiarch replacement	23.2	HCA-Only	12 m	DCS	No	Right	3 h 30 m
2	26	M	Valve sparing aortic root replacement + Ascending aortic + hemiarch replacement	17.9	RCP	17 m	DCS	No	Right	8 h 02 m
3	77	M	AVR + Ascending aortic + hemiarch replacement	24.9	ACP	20 m	DCS	No	Right	6 h 53 m
4	49	F	AVR + Ascending aortic + hemiarch replacement	27.1	ACP	14 m	FDNIRS-DCS	No	Right	4 h 26 m
5	78	M	CABG x 3 + AVR + Ascending aortic replacement	16.8	HCA-Only	25 m	DCS	No	Left	4 h 52 m
6	85	F	AVR + Pulmonary vein isolation + LAA ligation + Ascending aortic + hemiarch replacement	18.4	RCP	21 m	FDNIRS-DCS	Yes	Left	5 h 33 m
7	67	M	Ascending aortic + hemiarch replacement	22.0	ACP	20 m	FDNIRS-DCS	Yes	Right	3 h 57 m
8	59	F	Right pulmonary thormboendarterectomy + Left lower lobe wedge resection	19.6, 19.4	HCA-Only	19 m, 12 m	FDNIRS-DCS	Yes	Right	4 h 44 m
9	38	M	AVR + Ascending aortic + hemiarch replacement	18.2	RCP	22 m	FDNIRS-DCS	Yes	Right	5 h 30 m
10	45	M	Redo Sternotomy + total arch replacement	20.2	ACP	48 m	FDNIRS-DCS	Yes	Left	5 h 57 m
11	87	F	AVR + CABG x 1 + Pulmonary vein isolation + LAA ligation + Ascending aortic + hemiarch replacement	20.3	HCA-Only	29 m	FDNIRS-DCS*	Yes	Right	6 h 56 m
12	73	M	Redo Sternotomy + AVR + CABG x 4 + Ascending aortic + Zone I aortic arch replacement	18.8	ACP	47 m	FDNIRS-DCS*	Yes	Right	10 h 35 m

Table 1: Demographics of patient age and sex are given along with relevant parameters for the study. Circulatory arrest time refers to the length of time the normal blood flow was arrested (with or without cerebral perfusion). Patient #8 had two circulatory arrests. RCP: Retrograde Cerebral Perfusion with HCA; ACP: Antegrade Cerebral Perfusion with HCA. *Interference with the INVOS made it so FDNIRS data are only available discontinuously.

FDNIRS-DCS Device

For these measurements, we used a commercial combined FDNIRS-DCS system, MetaOx (ISS Inc. Champaign, IL). More device details can be found in Carp et al. (21). In four subjects, only the DCS component was used, and in the rest both DCS and FDNIRS data were acquired simultaneously (Table 1). The DCS component employed a single 35 mW, 850 nm light source and 8 photon counting detectors. The FDNIRS component included eight 2 mW light sources ranging between 670 and 830 nm in wavelength, and 4 photomultiplier detectors. The probe is shown in Figure 1.

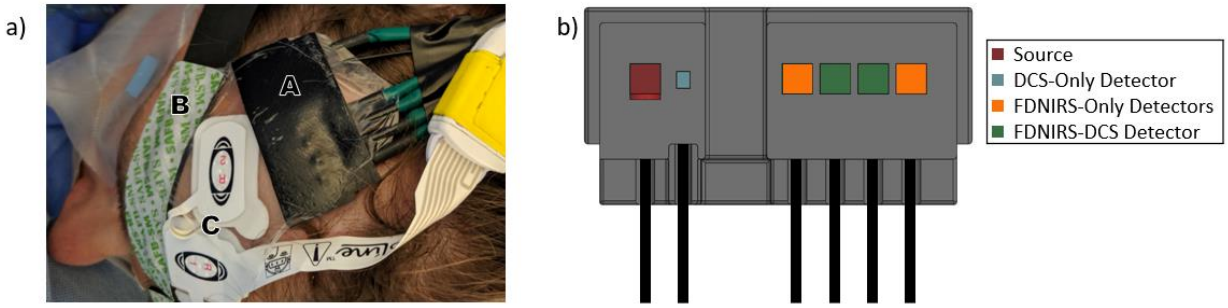

Fig 1: a) Photograph of our probe on a patient: A = FDNIRS-DCS, B = INVOS NIRS, C = processed EEG. b) Schematic of the FDNIRS-DCS probe. NIRS and DCS light sources are colocalized and diffused over a 3 mm spot diameter to meet ANSI standard irradiance limits. A DCS short separation detector (light blue) is located 5 mm from the source center, used to detect used to detect skin and scalp blood flow. Remaining DCS detector fibers (green) were located at 25 and 30 mm from the source fiber for higher sensitivity to cerebral blood flow. The short separation was necessary for data quality checking: both seeing lower CBF_i in the short separation and observing differences in relative signal changes between the short and long separations helps confirm that the longer separations are sensitive to blood flow beyond the scalp and skull layers. For patients that had DCS and FDNIRS measurements, the same probe also included NIRS fibers (green and orange). Patient #4 had four FDNIRS detectors at separations of 15, 20, 25, and 30 mm from the source. All other patients had FDNIRS fibers at separations of 20, 25, 30, and 35 mm from the source, as shown in the diagram.

Experimental Procedure

The optical probe was positioned on the patient's forehead after induction of general anesthesia. Other parameters were obtained from the Epic system such as electrocardiogram, pulse oximetry, cerebral oximetry (INVOS 5100c, Medtronic, Minneapolis MN; present in 7 patients), nasopharyngeal temperature and intra-arterial blood pressure. These signals were co-registered with our data at one point per minute resolution. The optical probe was secured against the right side of the patient's forehead, if possible. In three patients, cerebral oximetry and EEG were placed on the right side of the forehead in a way that did not leave enough room for the FDNIRS-DCS probe, so we placed the probe on the left side. We secured the probe several centimeters above the eyebrow and used surgical tape to secure the probe to the patient. To shield from ambient light, a soft black craft cloth was taped over the probe. In most cases, data collection began immediately after anesthesia induction and ended after chest closure (shortest: 3 h 30 m;

longest: 10 h 35 m; mean: 5 h 54m ± 1 h 58m). After data collection, we calibrated the FDNIRS detectors using three calibration blocks of known-optical properties.

Signal Processing and Analysis

Both DCS and FDNIRS (when available) signals were down-sampled to 0.2 Hz, followed by a 25-second moving average. Signal artifacts due to movement or interference from the INVOS NIRS were removed during preprocessing. For FDNIRS, we used the frequency-domain multi-distance method (22,23) to compute the absorption and scattering coefficients of measured tissue. From the absorption coefficient computed with at least 5 wavelengths, we estimated oxy- and deoxy- hemoglobin concentration (HbO_2 and HbR, respectively) and hemoglobin oxygen saturation (SO_2). For DCS, the semi-infinite medium correlation diffusion equation (16) was used to obtain an index of blood flow (BF_i) at short and larger source-detector separations (see supplementary material). To calculate BF_i for quantification of CA drop ratios, we used fixed absorption and reduced scattering coefficients, $\mu_a = 0.118$ cm^{-1} and $\mu_s' = 8.94$ cm^{-1}, obtained extrapolating to 850 nm the average coefficients obtained across all the subjects measured with FDNIRS.

Quantification of CBF_i and SO_2 changes through circulatory arrests

We quantified the CBF_i and SO_2 changes at CAs by calculating the average BF_i and SO_2 changes during a CA period with respect to that of a pre-CA period for each patient. We used the 2.5 cm DCS separation for CBF_i calculations. The duration of the pre-CA period was defined manually as a 1- to 10- minute window immediately before the CA onset during which BF_i, SO_2 and systemic physiology were stable. The CBF_i changes during HCA were calculated by averaging all values from 90 seconds after HCA/RCP/ACP start until the stop time. The 90-second delay was used to discard any artifacts at the beginning of the procedure. We measured the CBF_i overshoot at reperfusion times for HCA-only and RCP cases by averaging the values at the highest reperfusion peaks (there were multiple peaks in some cases where the surgeon asked to have the pump started and stopped several times) and comparing them to the settled CBF_i value, found by averaging a several-minute window directly after the peak.

For the subjects with FDNIRS and INVOS measurements, we quantified SO_2 changes by averaging one-minute pre-CA and the one-minute right before reperfusion. We normalized FDNIRS SO_2 drops with respect to time by dividing the total SO_2 drop by the number of minutes the CA procedure lasted.

Quantification of cerebral metabolic rate of oxygen and its relationship with temperature

For the quantification of $CMRO_2$ and its relationship with temperature, we used the data from the cooling and rewarming periods of the surgery, i.e. periods where temperature was not constant. To quantify $CMRO_{2i}$, we used the standard relation: $CMRO_{2i} = CBF_i(SaO_2 - SO_2)$. Because of the need for SO_2 in this analysis, only the subjects measured with both DCS and FDNIRS were included. Patients 11 and 12 were excluded because of the discontinuous nature of their FDNIRS measurements. In all subjects, arterial oxygenation (SaO_2) was maintained at 100% by the cardiopulmonary bypass.

For each subject, $CMRO_{2i}$ averages for cooling and rewarming periods were calculated separately. We averaged $CMRO_2$ values associated with up to seven evenly spaced temperature windows, from 20.5 °C to 34.5 °C. We normalized each patient's $CMRO_{2i}$ values with respect to the average $CMRO_{2i}$ in the window between 34.5-35.5 °C,

taken during each patient's rewarming period. Data with significant artifacts in CBF_i caused by CPB flow rate adjustments were excluded from calculations. To estimate the $CMRO_{2i}$ relationship with temperature, we fit a linear regression for all subjects' normalized $CMRO_{2i}$ (log scale) with respect to the mean temperature windows.

Statistical Analysis

Data normality was using a Shapiro-Wilk test and expressed as mean ± standard deviation. Statistical analyses were performed with a one-way ANOVA to compare the ratio of CBF_i and SO_2 during vs pre-CA among the three groups, followed by Dunnett T3 post hoc test for pairwise comparisons. Correlation analyses were performed with a Pearson test to reveal the relationship between $CMRO_{2i}$ and temperature. Statistical significance was evaluated by using a one tail *t*-distribution table with a 95% confidence interval. All tests were applied one-sided due to $CMRO_{2i}$ and temperature having a positive relation, and $p < 0.05$ was considered statistically significant.

Results

Our patient population and measurement characteristics are given in Table 1. All patients were in the region of hypothermia, with a mean minimum temperature of 19.9 ± 3.2 °C during CA and mean total CA time of 23.5 ± 11.7 minutes.

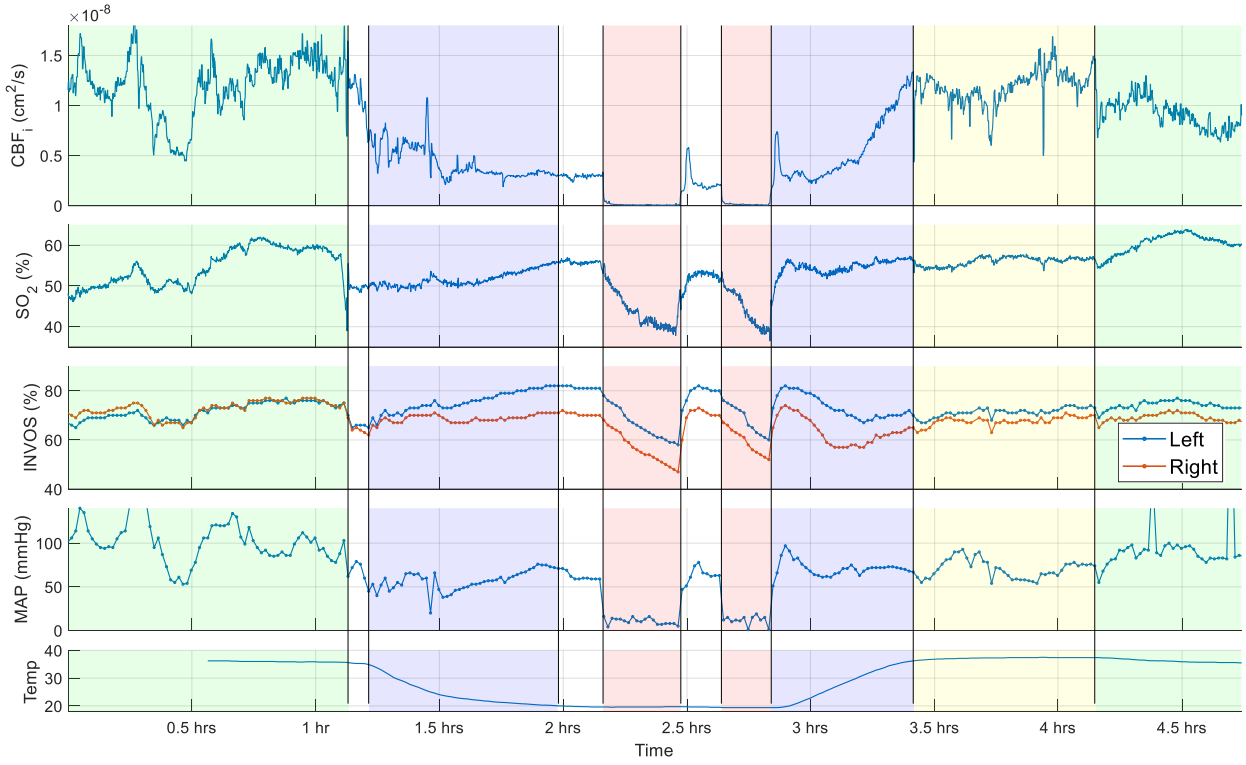

Fig. 2: Full measurement of a patient (ID#8) during a pulmonary thromboendarterectomy with two periods of HCA-only. CBF_i and oxygen saturation are measured by DCS and FDNIRS. The remaining three panels show the INVOS SO_2 measurements in both left and right sides, MAP, and brain temperature (measured with a nasopharyngeal probe) throughout the surgery. In sections shaded in light green the patient heart is circulating blood. In all other sections, the patient is on CPB.

CBF_i and SO_2 monitoring

Figure 2 shows a characteristic measurement of an HCA-only patient from start to finish (patient ID#8), with the major phases of the surgery labeled in colored sections. A wide range in CBF_i can be seen throughout the surgery, with large fluctuations before and after CPB and consistent high frequency "noise" corresponding to residual unfiltered heartbeat. Under CPB, CBF_i follows the temperature changes during the periods in which the body is cooled and rewarmed, while SO_2 remains consistent with the changes in $CMRO_2$. The most drastic change in CBF_i and SO_2 happens during circulatory arrest. In this subject, during the first period of CA, measured CBF_i dropped sharply from $0.30 \pm 0.017\times10^{-8}$ cm^2/s to $0.009 \pm 0.004\times10^{-8}$ cm^2/s, and SO_2 dropped gradually from 56.7 ± 0.3% to 39.3 ± 0.7%. In the second CA, measured CBF_i dropped sharply from $0.19 \pm 0.02\times10^{-8}$ cm^2/s to $0.012 \pm 0.005\times10^{-8}$ cm^2/s, and SO_2 dropped gradually from 53.1 ± 0.4% to 39.0 ± 0.9%.

Figure 3 shows the CBF_i and SO_2 time traces for an HCA-only case, an RCP case and an ACP case, focusing on the CA period.

CBF_i and SO_2 behavior at circulatory arrest

To examine cerebral perfusion changes during circulatory arrest, we quantified the ratios of CBF_i during versus pre-CA for each patient (Figure 4a). HCA-only patients saw that CBF_i dropped (down 95.5 ± 1.8%). The HCA with RCP patients had a drop in CBF_i as well (down 91.2 ± 3.3%), while HCA with ACP had a mean increase in CBF_i (up 14.3 ± 36.4%), with patient #7 receiving more than 50% more blood flow after the ACP started than during the pre-CA baseline. Note that measured CBF_i does not reach zero, even in HCA-only cases. While in normal physiological states, DCS measurements are driven by red blood cell movement. When blood flow is stopped, however, the residual thermal (Brownian) motion will result in a non-zero DCS perfusion estimate. This Brownian motion contribution is ~1% of the signal in normal conditions, so there is no significant contribution from Brownian motion to CBFi until it drops more than 90% from physiological levels.

There was a statistically significant difference among the three techniques as determined by one-way ANOVA ($F_{2,10} = 51.75$, $p = 0.001$). A Dunnett T3 post hoc test confirmed that the ratio of CBF_i during versus pre-CA was significantly lower in HCA-only (0.054 ± 0.009) and HCA with RCP (0.08 ± 0.03) cases, as compared to the HCA with ACP (1.11 ± 0.28) cases. The mean difference between the HCA-only and the HCA with ACP was statistically significant ($\bar{d}_D = -1.06$, $p = 0.003$). In addition, the HCA with ACP was statistically different than the HCA with RCP ($\bar{d}_D = 1.03$, $p = 0.003$). There was no statistically significant difference between the HCA-only and HCA with RCP ($\bar{d}_D = -0.03$, $p = 0.51$).

Figure 4b reports the total SO_2 drop and 4c reports the drop rates due to CA in all patients that had FDNIRS measurements. The SO_2 total drops and drops rates for HCA-only and HCA with RCP cases were similar, with total mean drops of 17.5 ± 3.9% in HCA-only and 13.0% in RCP, and mean drop rates of 0.93 ± 0.22% per min in HCA-only and 0.61% per min in RCP. Meanwhile, HCA with ACP mostly maintained SO_2 throughout the CA, with a mean total drop of 3.4 ± 1.82% and a mean drop rate of 0.17 ± 0.17% per min.

In quantifying the post-CA CBF_i overshoots, we found that the mean CBF_i overshoot was 2.6 ± 0.7 times higher in HCA-only cases and 2.9* times higher in RCP cases than the recovery values. We also quantified group averages for drops in the INVOS oximeter. The mean INVOS right side drop was 26 ± 9.8% in HCA-only, 12%* in RCP and 2 ± 6.0% in ACP cases. The mean INVOS left side drop was 27 ± 9.6% in HCA-only, 7%* in RCP and 10 ± 11.0% in ACP cases. We also report changes in mean arterial pressure (MAP) at CA (Table 2 in Supplementary).

Relationship between temperature and $CMRO_{2i}$

Figure 5 shows temperature dependency of $CMRO_2$ through the range of 18-35.5 °C (t_{10}, 0.005, $p = 0.001$) in 6 patients who had continuous FDNIRS measurements (Patients 4, 6-10). Each data point represents the average $CMRO_2$ values for the cooling/rewarm periods at the temperature value ± 1 °C. As expected, $CMRO_2$ was strongly positively related to temperature, r (62) = 0.85, $p < 0.01$.

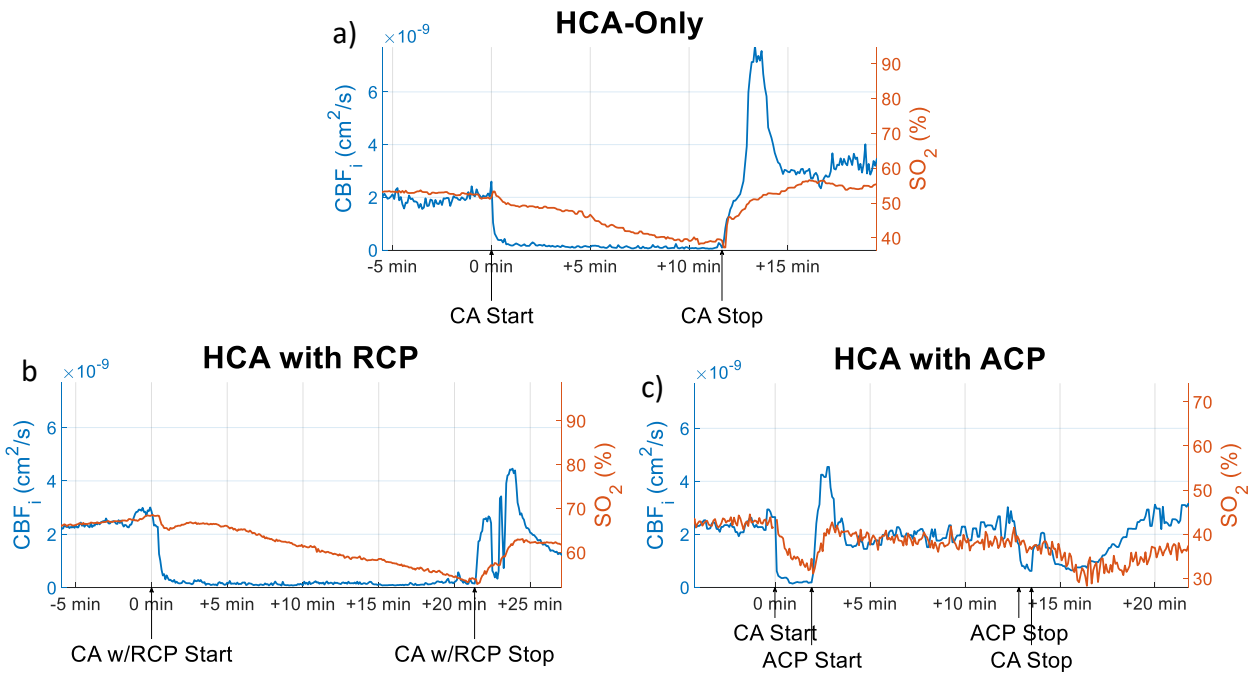

Fig. 3: a) CBF_i and SO_2 data from patient #8, during the second deep hypothermic circulatory arrest with no extra perfusion. CBF_i dropped 93.7 ± 2.7% within the first minute of CA. The patient's SO_2 dropped by 14.1 ± 1.0% over the 12-minute period of circulatory arrest (1.18 ± 0.08% per minute). b) Patient #6, who underwent DHCA with RCP. CBF_i dropped 93.0 ± 2.6% within the first minute of HCA. SO_2 dropped at a similar rate (0.66 ± 0.03% per min) as the HCA-only patient and dropped by SO_2 dropped by 23.0 ± 0.7% after 20 minutes of CA. c) Patient # 4, who underwent HCA with ACP. CBF_i dropped by 91.9 ± 0.3% and SO_2 dropped at a rate of 1.95 ± 0.008% per min between CA start and ACP start. The higher drop rate of SO_2, in this case, is likely due to higher cerebral metabolic activity, being at a higher temperature (27.1°C). Both CBF_i and SO_2 quickly recovered to pre-CA values after ACP start and were maintained until ACP stop (CBF_i dropped by 11.1 ± 2.8%; SO_2 drop rate 0.39 ± 0.08% per min). It is noticeable that cerebral perfusion does not increase as expected from an RCP procedure. This was indicated by CBF_i more promptly than SO_2 signal.

* No error is shown as there are ≤ 2 patients in this sample

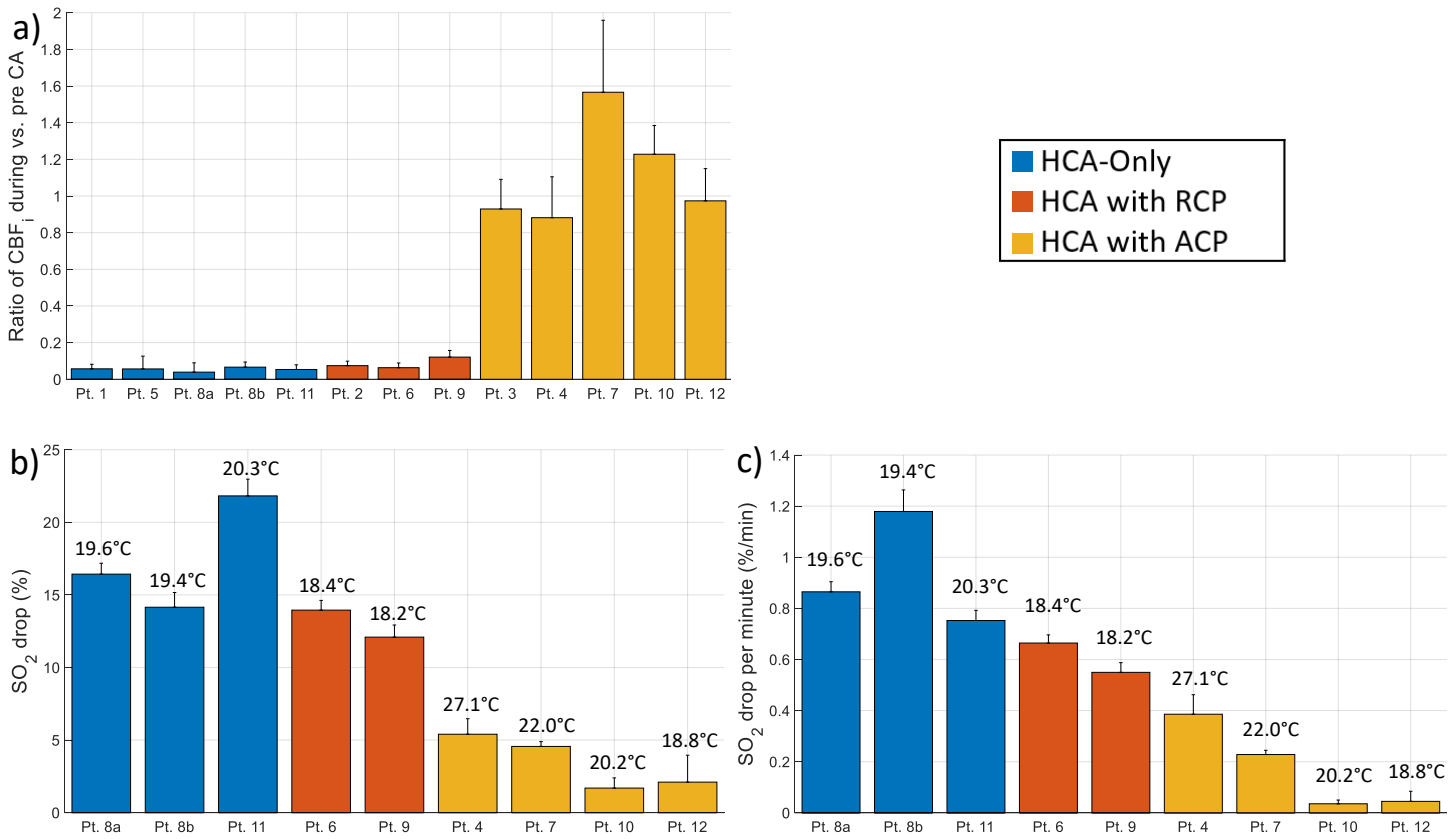

Fig. 4: a) The ratios of CBF_i during CA versus pre-CA onset. During CA was defined as the average from one minute into CA to the CA stop time. Pre-CA interval was identified visually as a one to ten-minute period immediately before CA start where cerebral flow and systemic physiology were level. b) Percent Drop of SO_2 from pre-CA to end of CA as measured with FDNIRS-DCS device. Values were averaged for 30-60 seconds for both pre-CA and during CA values. c) Drop rate of SO_2 during CAs. Time intervals were determined using hospital records and are precise to the minute.

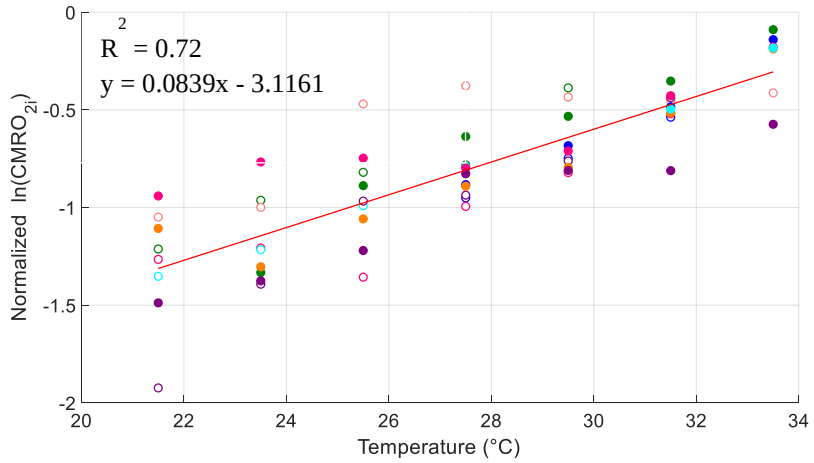

Fig. 5: Log of relative $CMRO_2$ versus temperature. Open markers indicate cooling periods and filled markers represent rewarming periods. Each patient's $CMRO_2$ values are normalized with respect to average $CMRO_2$ between 34.5-35.5 °C during patient rewarming. *Correlation between $CMRO_2$ and temperature are statistically significant at the 0.01 level.

Correlations

Averaged across all subjects, the average correlation between CBF_i and MAP was 0.29 ± 0.36, between CBF_i and SO_2 was -0.15 ± 0.41 and between our continuous FDNIRS SO_2 measurements and the INVOS was 0.82 ± 0.14.

Discussion

This is the first report using FDNIRS-DCS to evaluate the efficacy of commonly used brain protection strategies during HCA in adult cardiac surgery procedures.

Since DHCA was first successfully used during aortic arch surgery over thirty years ago, clinical outcomes have significantly improved (7). The development of adjunct cerebral perfusion techniques has allowed cardiac surgeons to perform more complex operations that require longer durations of CA. However, aortic arch surgery is still associated with a 5-10% risk of clinically significant neurologic injury, and much higher risk of subclinical neurological insult (24). The lack of reliable intraoperative brain monitoring techniques remains a limitation as we try to determine the best brain protection strategy during CA. EEG, TCD and NIRS have all been used, but none of them can reliably provide a measure of cerebral protection, which is essential during hypothermic CAs with ACP or RCP. This leads us to use DCS, which gives us a direct measure of blood flow index, is easy to use and allows for continuous monitoring.

CBF_i and SO_2 in HCA-only and HCA with RCP

RCP was introduced in aortic arch surgery to provide another layer of brain protection in addition to hypothermia. It is reported to reduce stroke risk by flushing out air or debris from the brain that may enter during the manipulation of the aorta and head vessels (7). The efficacy of RCP to provide sufficient brain perfusion has been challenged by Ehrlich et al., who showed (using microsphere calculations) that in pigs undergoing HCA with RCP, less than 13% of the perfusate from RCP makes its way out of the arteries, with negligible flow reaching the brain (25). Our DCS measurements showed that brain flow during RCP was indistinguishable from that of HCA-only patients. This finding is consistent with the pig study, and the negligible amount of blood flow we detected further questions the efficacy of RCP as a neuroprotective method.

Another interesting finding of our study is the detection of an overshoot in cerebral blood flow in the HCA-only and the RCP groups immediately after the conclusion of circulatory arrest (Figure 3). This may be due to loss of cerebral autoregulation in these group of patients and may put them at a higher risk of reperfusion injury on resumption of CPB flow. There are increasing data indicating that cerebral hyper-perfusion is as harmful as hypoperfusion; DCS could warn not only about low but also dangerously high cerebral flow levels (26). DCS was uniquely able to recognize brain hyper-perfusion post-CA as this phenomenon was not reflected in SO_2 readings, which gradually returned to pre-HCA levels.

Combined, DCS and FDNIRS (which is highly valuable in monitoring progressive ischemia during CA) can provide useful information during CA, alerting the clinical team whether the brain is perfused as expected, and when is it time to stop CA.

CBF_i and SO_2 in HCA with ACP

Because it provides oxygenated blood in a physiological manner, ACP has become more popular than RCP over the past fifteen years. Most surgeons choose the right axillary artery for ACP, titrating ACP flow to a pressure of 50-70 mmHg and flow of 6-10 ml/kg/m to provide adequate brain perfusion (26). However, these established ACP flow rates are largely based on the empiric data and retrospective studies, with no direct measurements supporting it. Also, older patients may have a partially degraded circle of Willis, potentially compromising contralateral brain oxygenation (27). If the contralateral SO_2 levels drop during CA, the clinicians may ask to raise perfusion pressure or increase flow to facilitate left hemisphere perfusion. While this may be helpful in the setting of an intact circle of Willis, in others this can raise intracranial pressure and potentially cause ipsilateral brain injury without improving contralateral perfusion. DCS could potentially be a valuable tool to not only warn if flow is not reaching the contralateral side of the brain, but also to detect dangerously high flow ipsilaterally. In the current study, the DCS probe was placed only on the right side in all but one patient in the ACP group (ID#10), but we saw no flow reduction during CA. A bilateral measurement of CBF_i would allow monitoring of ACP efficacy in both brain hemispheres and help identify patients that will benefit from institution of bilateral cerebral perfusion.

Because of the heterogenicity of patients undergoing aortic arch surgeries, we can expect that ACP flow rates should be individualized for each patient. Further study is needed to confirm that measuring brain blood flow with DCS could provide better brain protection and allow individualization of ACP flow rates during CA.

Study Limitations and Additional Comments

A limitation of our study is the lack of bilateral measurements comparing hemispheres, which is particularly of interest to ensure bilateral brain perfusion during unilateral ACP.

It is worth noting the disparity between the SO_2 values measured by the INVOS versus FDNIRS. The INVOS SO_2 shows higher values and drops than the FDNIRS values, likely because of the strong assumptions made with the continuous wave (CW) device (28). Nevertheless, the correlation between the two measurements is very high.

A challenge in using DCS is ensuring that the longer separations are sensitive to cerebral flow. In all data sets we were able to identify periods of short separation (5 mm) changes that had no effect on long separations (25 and 30 mm). Also, in ten of our twelve measurements, the long separations consistently showed larger BF_i values than the short separation, with some periods reporting almost two times the value. We therefore believe that our longer separations are sensitive to the brain physiology. For the two measurements (IDs #1 and 6) where the short separation BF_i was higher, we believe the probe may have been placed directly over or near to a superficial vessel, causing short separation DCS to report higher than normal flow. The conclusions of our data analysis did not change based on the inclusion or exclusion of these two data sets, so we kept both in our analysis.

Conclusions

We conclude that DCS reliably measures cerebral blood flow index and uniquely identifies periods of brain hypoperfusion and hyperperfusion during cardiac surgical procedures using circulatory arrest. We further state that

RCP should be investigated further for proof of efficacy, or lack thereof. Overall, DCS alone or combined with NIRS can potentially guide brain protection to help clinicians achieve optimal brain perfusion.

Acknowledgments

The authors thank Zack Starkweather for designing the optical probes and Adriano Peruch for device designs. Also, thank you to Juliette Selb, Melissa Wu and Vidhya V. Nair for their contributions to data acquisition.

Author contribution statement

Conceived of and designed the study: AIZ, KK, PF, PYF, SAC, MAF, JZQ; Acquired data: AIZ, KK, PF, PYF, SAC; Wrote analysis software: AIZ, PF, FOE; Data analysis and figures: AIZ; Provided valuable advice for analysis: KK, PF, JS, FOE, ASJ, SAC, MAF; Statistical analysis: KK; Wrote the manuscript: AIZ, KK, MAF, JZQ; Contributed to writing the manuscript: all authors; Performed or helped with surgical procedures: ASJ, DEC, TMS, SM, JZQ. Final approval of the version to be published: all authors.

Disclosure/conflict of interest

This work is supported by NIH R01GM116177 and R01HD091067 (MAF), R01NS100750 (SC) and CONACYT 2018-000007-01EXTV (FOE). MAF has a financial interest in 149 Medical, Inc., a company developing DCS technology for assessing and monitoring cerebral blood flow in newborn infants, and in Dynometrics, Inc., a company that makes devices that use NIRS technology for athletes to evaluate muscle performance. MAF's interests were reviewed and are managed by Massachusetts General Hospital and Partners HealthCare in accordance with their conflict of interest policies.

Supplementary Material

Supplementary material for this paper can be found at the journal website: http://journals.sagepub.com/home/jcb

References

1. Mezrow CK, Sadeghi AM, Gandsas A, Dapunt OE, Shiang HH, Zappulla RA, et al. Cerebral effects of low-flow cardiopulmonary bypass and hypothermic circulatory arrest. The Annals of thoracic surgery. 1994 Mar;57(3):532–9; discussion 539.
2. Griepp EB, Griepp RB. Cerebral consequences of hypothermic circulatory arrest in adults. Journal of cardiac surgery. 1992 Jun;7(2):134–55.
3. Svensson LG, Crawford ES, Hess KR, Coselli JS, Raskin S, Shenaq SA, et al. Deep hypothermia with circulatory arrest. Determinants of stroke and early mortality in 656 patients. The Journal of thoracic and cardiovascular surgery. 1993 Jul;106(1):19–31.
4. Griepp RB, Stinson EB, Hollingsworth JF, Buehler D. Prosthetic replacement of the aortic arch. The Journal of thoracic and cardiovascular surgery. 1975 Dec;70(6):1051–63.
5. Greeley WJ, Kern FH, Meliones JN, Ungerleider RM. Effect of deep hypothermia and circulatory arrest on cerebral blood flow and metabolism. The Annals of thoracic surgery. 1993 Dec;56(6):1464–6.
6. Englum BR, He X, Gulack BC, Ganapathi AM, Mathew JP, Brennan JM, et al. Hypothermia and cerebral protection strategies in aortic arch surgery: a comparative effectiveness analysis from the STS Adult Cardiac Surgery Database. European journal of cardio-thoracic surgery : official journal of the European Association for Cardio-thoracic Surgery. 2017 Sep;52(3):492–8.
7. Geube M, Sale S, Svensson L. Con: Routine Use of Brain Perfusion Techniques Is Not Supported in Deep Hypothermic Circulatory Arrest. Journal of Cardiothoracic and Vascular Anesthesia [Internet]. 2017;31(5):1905–9. Available from: http://dx.doi.org/10.1053/j.jvca.2017.02.024
8. Itagaki S, Chikwe J, Sun E, Chu D, Toyoda N, Egorova N. Impact of Cerebral Perfusion on Outcomes of Aortic Surgery: The Society of Thoracic Surgeons Adult Cardiac Surgery Database Analysis. The Annals of thoracic surgery. 2020 Feb;109(2):428–35.
9. Mizrahi EM, Patel VM, Crawford ES, Coselli JS, Hess KR. Hypothermic-induced electrocerebral silence, prolonged circulatory arrest, and cerebral protection during cardiovascular surgery. Electroencephalography and clinical neurophysiology. 1989 Jan;72(1):81–5.
10. Shin'oka T, Nollert G, Shum-Tim D, du Plessis A, Jonas RA. Utility of near-infrared spectroscopic measurements during deep hypothermic circulatory arrest. The Annals of thoracic surgery. 2000 Feb;69(2):578–83.
11. Purkayastha S, Sorond F. Transcranial Doppler ultrasound: technique and application. Seminars in neurology. 2012 Sep;32(4):411–20.
12. Naqvi J, Yap KH, Ahmad G, Ghosh J. Transcranial Doppler ultrasound: a review of the physical principles and major applications in critical care. International journal of vascular medicine. 2013;2013:629378.

13. Dehaes M, Cheng HH, Buckley EM, Lin P-Y, Ferradal S, Williams K, et al. Perioperative cerebral hemodynamics and oxygen metabolism in neonates with single-ventricle physiology. Biomedical optics express. 2015 Dec;6(12):4749–67.

14. Durduran T, Zhou C, Buckley EM, Kim MN, Yu G, Choe R, et al. Optical measurement of cerebral hemodynamics and oxygen metabolism in neonates with congenital heart defects. Journal of biomedical optics. 2010;15(3):37004.

15. Buckley EM, Hance D, Pawlowski T, Lynch J, Wilson FB, Mesquita RC, et al. Validation of diffuse correlation spectroscopic measurement of cerebral blood flow using phase-encoded velocity mapping magnetic resonance imaging. Journal of biomedical optics. 2012 Mar;17(3):37007.

16. Durduran T, Choe R, Baker WB, Yodh AG. Diffuse Optics for Tissue Monitoring and Tomography. Reports on progress in physics Physical Society (Great Britain). 2010 Jul;73(7).

17. Busch DR, Rusin CG, Miller-Hance W, Kibler K, Baker WB, Heinle JS, et al. Continuous cerebral hemodynamic measurement during deep hypothermic circulatory arrest. Biomedical optics express. 2016 Sep;7(9):3461–70.

18. Ferradal SL, Yuki K, Vyas R, Ha CG, Yi F, Stopp C, et al. Non-invasive Assessment of Cerebral Blood Flow and Oxygen Metabolism in Neonates during Hypothermic Cardiopulmonary Bypass: Feasibility and Clinical Implications. Scientific reports. 2017 Mar;7:44117.

19. Baker WB, Balu R, He L, Kavuri VC, Busch DR, Amendolia O, et al. Continuous non-invasive optical monitoring of cerebral blood flow and oxidative metabolism after acute brain injury. Journal of cerebral blood flow and metabolism : official journal of the International Society of Cerebral Blood Flow and Metabolism. 2019 Aug;39(8):1469–85.

20. Lu H, Xu F, Rodrigue KM, Kennedy KM, Cheng Y, Flicker B, et al. Alterations in cerebral metabolic rate and blood supply across the adult lifespan. Cerebral cortex (New York, NY : 1991). 2011 Jun;21(6):1426–34.

21. Carp SA, Farzam P, Redes N, Hueber DM, Franceschini MA. Combined multi-distance frequency domain and diffuse correlation spectroscopy system with simultaneous data acquisition and real-time analysis. Biomedical optics express. 2017 Sep;8(9):3993–4006.

22. Fantini S, Franceschini MA, Gratton E. Semi-infinite-geometry boundary problem for light migration in highly scattering media: a frequency-domain study in the diffusion approximation. Journal of the Optical Society of America B. 1994;11(10):2128.

23. Fantini S, Franceschini MA, Fishkin JB, Barbieri B, Gratton E. Quantitative determination of the absorption spectra of chromophores in strongly scattering media: a light-emitting-diode based technique. Applied optics. 1994 Aug;33(22):5204–13.

24. Leshnower BG, Rangaraju S, Allen JW, Stringer AY, Gleason TG, Chen EP. Deep Hypothermia With Retrograde Cerebral Perfusion Versus Moderate Hypothermia With Antegrade Cerebral Perfusion for Arch Surgery. The Annals of thoracic surgery. 2019 Apr;107(4):1104–10.

25. Ehrlich MP, Hagl C, McCullough JN, Zhang N, Shiang H, Bodian C, et al. Retrograde cerebral perfusion provides negligible flow through brain capillaries in the pig. The Journal of thoracic and cardiovascular surgery. 2001 Aug;122(2):331–8.

26. Halstead JC, Meier M, Wurm M, Zhang N, Spielvogel D, Weisz D, et al. Optimizing selective cerebral perfusion: deleterious effects of high perfusion pressures. The Journal of thoracic and cardiovascular surgery. 2008 Apr;135(4):784–91.

27. Zaninovich OA, Ramey WL, Walter CM, Dumont TM. Completion of the Circle of Willis Varies by Gender, Age, and Indication for Computed Tomography Angiography. World neurosurgery. 2017 Oct;106:953–63.

28. Kleiser S, Nasseri N, Andresen B, Greisen G, Wolf M. Comparison of tissue oximeters on a liquid phantom with adjustable optical properties. Biomedical optics express. 2016 Aug;7(8):2973–92.